Micro-Grid Inrush Current Stability Analysis

Alexander Matthee
University of Twente
Enschede, The Netherlands
alex.matthee@utwente.nl

Niek Moonen
University of Twente
Enschede, The Netherlands

Frank Leferink
University of Twente, Enschede
Thales, Hengelo
The Netherlands

***Abstract*—Transient currents can severely impact the operation of weak or islanded grids. Inrush current electromagnetic compatibility challenges, due to their unpredictable and intermittent nature, are very difficult to identify. Using multi-point synchronised measurements, analysis is performed on an inverter. The supply powers various loads that are observed during cold start as well as under load switching conditions. Inrush event triggered failure probability is linked to non linear and average load levels.**

***Index Terms*—Generator efficiency, Multi-point measurement, Electromagnetic interference, Smart grids,**

I. Introduction

A rising concern is the electromagnetic compatibility (EMC) challenge associated with inrush currents and harmonics caused by switching power electronics converter (SPECs) and other non-linear devices [1], [2]. Switching of motor loads generally exceed nominal power during start up or acceleration phase that may last for milliseconds or longer depending on ramp up times [3]. To mitigate these effects islanded power supplies, whether generator or inverter, are often designed with a margin of safety over the rated load power to provide resilience against short-time load spikes which is also dependent on load type [3]. There appears to be some variance in the recommended buffer, ranging from 50% to 500%. This over capacity margin does not only concern reliability of a system but inherently results in increased costs of acquisition, running efficiency and maintenance. With increase in supply nominal power, a larger size footprint and or weight is usually a result. A usual case would be to multiply the max supply power in volt-amps by 0.8 to compensate for power factor and another 0.8 as a safety factor to achieve the max power load in kilowatts. For example, a vehicle carrying a generator with 40 kVA rated power supplying a complex microgrid with an average load of 23 kW [4]. Modern non-linear loads with many discharged capacitors charging up during switching events somewhat void the safety factor capacity of isolated supplies causing faults often intermittent in nature. Such is the case in hospitals testing backup electrical systems, which are by law required for surgery or life support systems. Failure on cold start due to inrush currents of multiple non-linear devices simultaneously charging up capacitors is a major concern [5].

ETOPIA project research is funded by the European Union's Horizon 2020 research and innovation programme under the Marie Sklodowska-Curie grant agreement No 812753.

Diagnosis of these problems can be challenging, especially in large complex systems. Compliance with standards offers some form of protection but this is often not adequate considering the perpetuation of system reliability issues. It is stated in [6] that the surge or inrush current should not exceed a maximum of 10 times the current of the rated equipment. It also states that individual loads less than 1 kW are exempt from this, which essentially means no requirement to limit inrush currents. This is concerning since the last two decades have followed a trend of smaller and more efficient devices. Hence it can be assumed more devices fall in this less than 1 kW group. Power consumption of many devices are decreasing and non-linear devices are dominating the market. Since these devices, such as light emitting diode (LED) lighting, actually use a small amount of power individually but are usually connected in large banks. Therefore the effect is constructive. A large number of small electromagnetic interference (EMI) sources have shown to be problematic [7], [8]. In short, there is a misconception of the negative effects of inrush current due to large amounts of non-linear devices connected to a supply with guidelines to optimal size capacity varying vastly.

Besides over-sizing of supply sources other techniques can be an effective mitigating factor against harmful EMI. According to [9] the grid impedance can have an effect on false tripping of islanded systems with a higher impedance increasing the probability of interference. Interesting to note is the findings that certain combinations of harmonic components can have a greater effect on system stability compared to one large harmonic component, such as the 3rd and 5th. Control techniques can be effective for compensating these harmonics in inverters [10]. Injection of current or voltage to increase the immunity to harmonics or inrush interference events have been proposed [11], [12]. An Established method to smooth out current transients and harmonics would be the implementation of power line filters [13]. Adding inductors and capacitors can be effective but may not always be a comprehensive solution. The costs and size of the components may become a significant factor and in certain applications where the size and weight of the added components may not be practical [14]. Multi-supply or hybrid micro-grid configurations may improve immunity to conducted EMI by implementing an inverter and/or generator in combination with a battery [15]. In this paper an isolated grid has been set up with a commercial off the shelf inverter and loads illustrated in Fig. 1. The representation is intended to

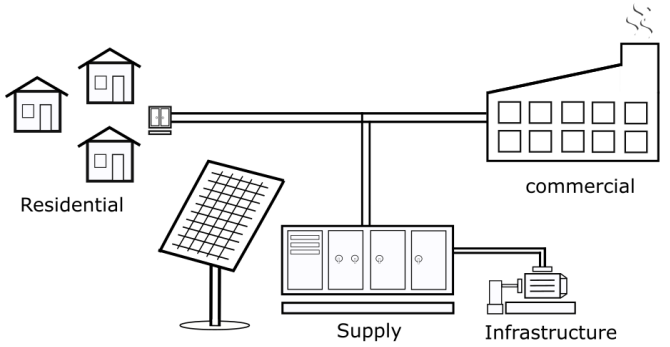

Fig. 1: Micro-grid component diagram

mimic conditions for in-situ measurements of a small remote village which includes a commercial component. The solar PV powered grid supplies a local water pump as well as a residential and commercial component with a mixture of non-linear and linear loads. The chosen loads include common lighting as well as heating, and some motor loads. The system voltages and currents are measured in multiple points with synchronisation between all measured nodes using the system described in [16]. This method enables all current and voltage time domain wave-forms to be directly compared. Sources and consequences of switching transients or inrush currents are traced and analysed. Using realistic loading conditions coupled to a finite supply inverter, the factor of risk is determined and failure cases examined. Practical solutions are suggested which may increase immunity to inrush EMI events. In Section II the setup and measurement approach is detailed. An inverter failure event and contributing factors is analysed in Section III and a statistical analysis is done on multiple inrush events with various load levels in Section IV.

II. Micro-Grid Setup Overview

The setup includes a Cinergia grid emulator which represents an off-grid Solar inverter with rated power of 5 kVA running in independent mode. The Cinergia supply overload limits are specified as 10 min at 125% or 1 min at 150%. A Cinergia electronic load is used which is a sinusoidal linear variable load. This represents a variable frequency drive (VFD) powering a water pump for a local village in a remote area. The residential component consists of LED lighting, a resistive heater and a small water pump. The water pump with dimmer as well as the LED bank are known disruptive loads with large inrush and harmonic current draw [17]. The commercial component includes a motor load. The loads and power rating are specified in Table I with a diagram for connection of loads in Fig. 2. Each load is controlled individually via a relay. The relays are activated using GPIO pins from a Raspbery Pi 4 (RP4) device and controller module. A script running from a laptop computer controls the RP4 GPIO pins. This allows switching loads independently or in sync with accurate control. A high inrush case scenario test is performed switching loads (1,2,3,4) simultaneously. Since the supply voltage phase firing angle at which the non-linear loads are energised heavily influences the inrush current, the relays are switched in a sequence to ensure that the non-linear loads energise on a peak. The relay will close the circuit at a specified time instant and continue for 1.5 s. The circuit is then opened for 1.5 s to allow the capacitors to discharge. The circuit is closed again in 1.5 s + 1 ms offset iterating for 10 cycles repeating the pattern.

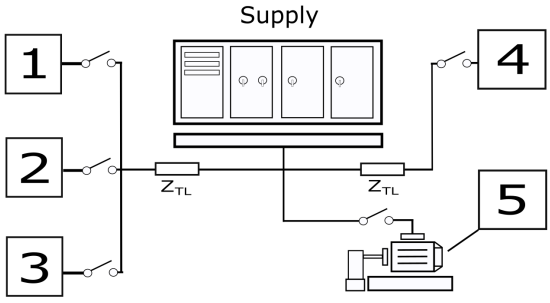

Fig. 2: Load setup diagram

This results in an inrush event near the peak of the voltage cycle for each test procedure. Loads are energised in two different approaches in separate test cases. One test case procedure with a no load "cold start" and another with initial linear load of 1.8 kW. The former represents initial system start with no loads active to full load active on a single switch event. This results in the largest inrush currents on a switch event. The latter represents a system running with active loads and switching events occurring during operation.

TABLE I: Branch loads

Load	Description	Nominal Power (W)
(1)	Resistor bank (heater)	1800
(2)	LED light bank (32x2W + 5x11W)	119
(3)	Water pump with dimmer	130
(4)	Motor load (drill)	850
(5)	Variable electronic load	0 $\backsim$ 2000

III. Cold start measurement results

Energising all the loads simultaneously near the voltage peak is considered, in terms of inrush current, the worse case scenario with regards to peak instantaneous power draw. In Fig. 3 one such measurement is shown with all loads energised near the peak of the supply voltage waveform indicated at 11506 ms. The voltage waveform is distorted by the 80.1 A current draw of all combined loads and the inverter subsequently fails with an over-current protection fault. The system shuts down, the fault codes must be cleared and manually restart is required. The exact current levels at which the system fails is unclear as the failure appears to be determined by various factors. More information is provided in Section IV. The total nominal load connected to the supply is 2.865 kW. This equates to a 57% of load rated power of the supply or from the perspective of a over capacity margin, a system rated at $\pm$ 174% of nominal load.

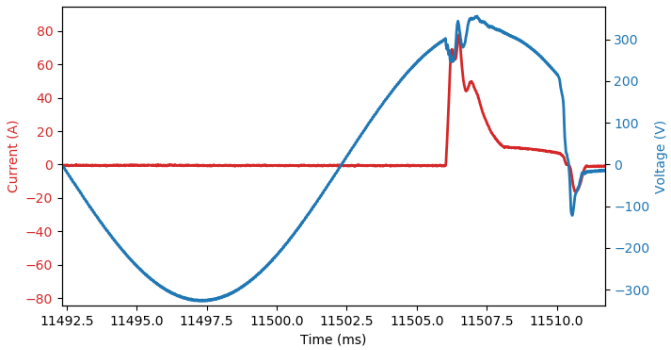

Fig. 3: Voltage and Current during inrush phase resulting in supply overload

The instantaneous power during this event is significant, shown in Fig. 4. The power peaks at 26.2 kW and last for nearly 5 ms exceeding the rated power (5 kVA) of the supply for 1.8 ms. The peak power consumption for this event is at 524% ratio of supply nominal power. This event activates the protection systems on the supply and the grid fails, requiring manual restart and fault clearing. Using the stipulated loads the system is exposed to risk of failure on switching events. The extent of the risk is not determined as system failure is not consistent nor has clearly defined limits. Gaining more data points, some patterns may start to emerge. This is investigated in Section IV.

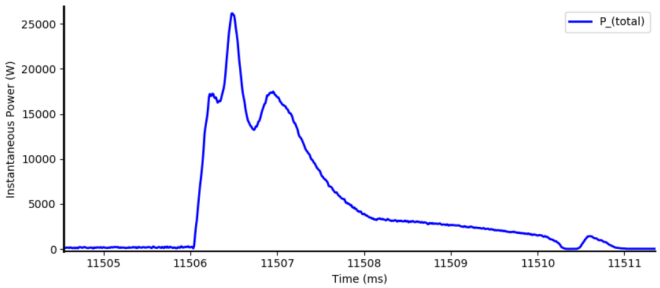

Fig. 4: Instantaneous Power draw during inrush

IV. Running Switching Events Measurement Results

Running multiple inrush switching tests for various load combinations yields some interesting results. In Fig. 5 the currents drawn during the inrush test procedure is shown with a zoomed in plot added for the first inrush event. The test case in this execution involved loads (1,2,3,4), a combination of SPECs and a linear load. It can be seen that the energising of the loads results in large current draws from the non-linear loads and constant amplitude from the linear as expected. The deviation of inrush current draws is determined by the voltage firing angle at which the loads are activated. In this test case this varies for every activation and thus peak currents can deviate drastically. The final inrush event results in failure of the supply (The same failure case data analysed in Section III and Fig. 3).

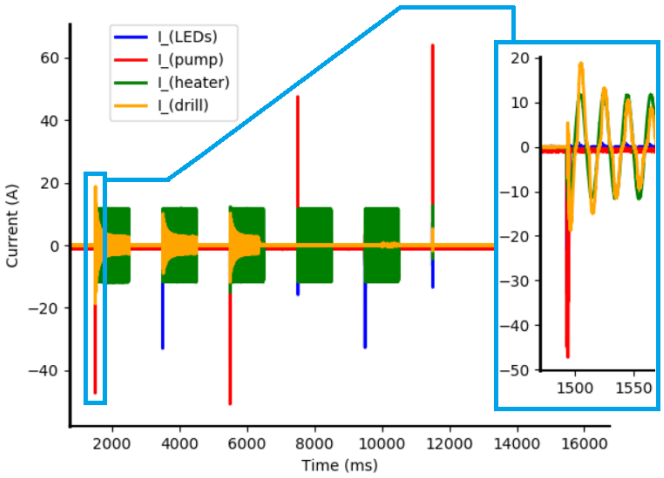

Fig. 5: Individual load currents during inrush test for cold start

These currents represent the current of each load individually, but of course the supply current will result in a sum of load currents shown in Fig. 6. The interesting point is that the highest peak current did not result in supply failure. The peak measured current is approx. 126 A peak and the event which resulted in the failure peaks at 77 A.

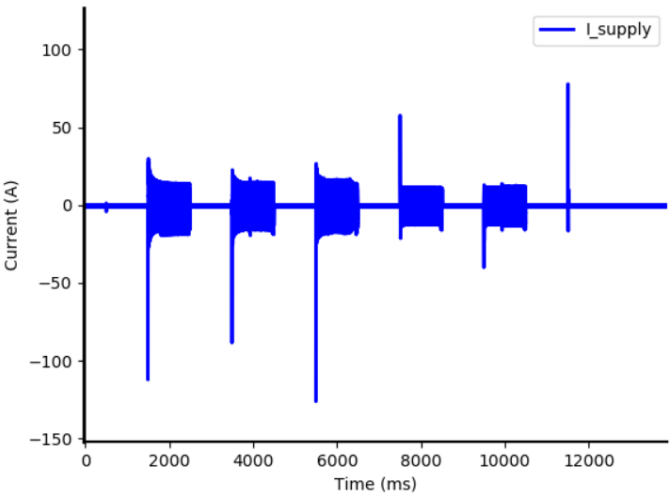

Fig. 6: Supply current during inrush test prodecure

Rerunning the switching event test multiple times allow some patterns to emerge. Each test run causes either 10 inrush events or the number until the supply fails. During the test run 257 inrush events are documented of which 17 caused system failure. The remainder of 240 events did not result in critical system interference. Superimposing all the time domain current waveforms in a single plot, with an opaque line plot, shows distributions of current behaviour during inrush events. The darker regions, where multiple waveforms re-occur, shows repetitive measurement data and lighter plot lines less probable measurements as a probability density plot. The data is shown in Fig. 7 with current measurements mirrored

and split between pass (blue) in top section of the plot (no system shutdown) and fail (system shutdown) on the bottom in red.

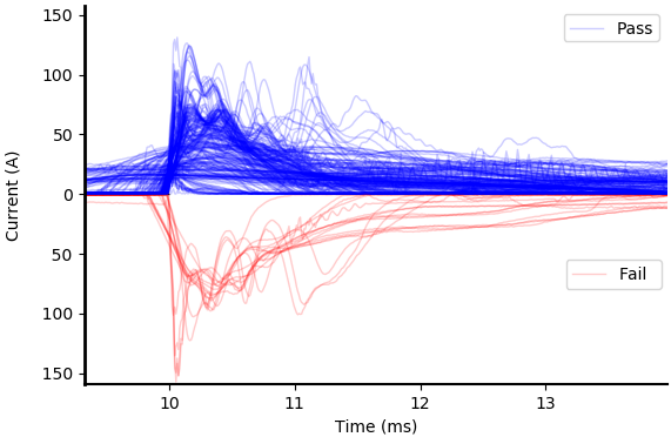

Fig. 7: Instantaneous Power draw during inrush

This shows behaviour that the events which cause system failure cannot always be distinguished from those that do not. The inrush events which cause failure have mostly a high current draw and relatively long duration but some events which do not cause failure may in some instances appear more severe than some which case failure. The observation is that non-failure events may have high current peak draws but inrush events, which cause failure, have high current draws. Looking further into firing angle of the inrush events, a plot is shown in Fig. 8. The plot consists of 257 time domain voltage waveforms superimposed on one another and phase shifted to be aligned. The blue line represents the voltage waveform once again opaquely plotted as well as red opaque lines (blue dominates the due to larger amount of ”pass” waveforms in dataset). The green markers represent the instants on the voltage phase which an inrush event occurred which did not cause a system failure. The red markers indicate the phase firing angle which resulted in a system failure.

From this it can be deducted that the firing angle on the voltage waveform may not always result in failure on the peak of the voltage waveform when inrush occurs with similar loading conditions. Although the red markers indicate that the highest probability exists near or just before the peak of the sinusoidal voltage waveform. This highlights the problem that inrush current failures are difficult to diagnose on systems. More so on more complex systems. Using a system with a fixed set of loads may work for a certain period of time and fail at intermittent intervals. Furthermore, as stated previous, the loading of the supply effects the probability of supply interference. A higher component of non-linear loads as well as higher nominal load compared to the rated load of the supply increases the risk of EMI. For this test setup known disruptive loads such as LED light banks and a water pump with dimmer connected. A concerning discovery is that even with only the two highly disruptive (LEDs and water pump)

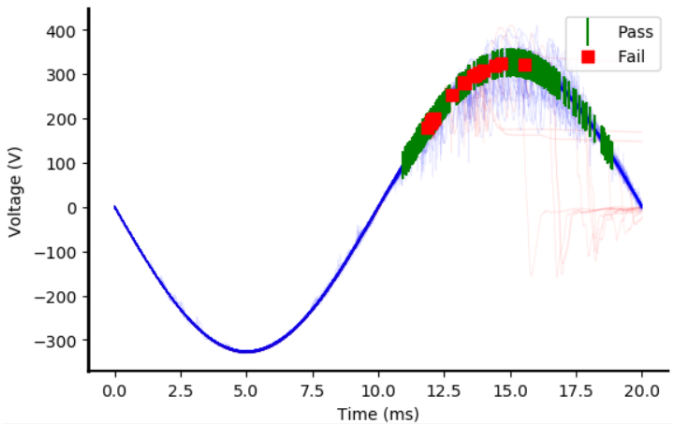

Fig. 8: Probability plot of inrush event result superimposed on voltage waveforms

loads connected inrush currents could still cause failure of the supply. The nominal power of these two loads are cumulatively 250 W and would be expected to not disrupt a supply rated at 5 kVA. Shown in Table II is the connected loads for two different load profiles during the inrush test procedures. The ”full” load equals a system designed at 174% rated power of the loads. The test with only the disruptive non-linear loads connected is equivalent to a supply design of 20000% of rated load.

TABLE II: Load vs Failure probability

Case	Load (kW)	Capacity (%)	Fail	Pass	Fail Rate (%)
full	2.9	174	7	69	9.2
non-linear	0.25	20000	6	104	5.4

From Table II it can be seen that the higher average load in this specific case does indeed increase the probability of interference but not by any measure linearly proportional. Furthermore, connecting the Cinergia Electronic load representative of the ”VFD” in the microgrid emulation as a replacement for the 1.8 kW resistive heater resulted in minor deviation in failure rate from the similar linear load. In fact the failure rate is slightly reduce which may be due to a smaller dataset or due to the presence of the extra power line filter connected to the circuit as well as the precharging function of the electronic load before activation. Usually during cold start system switch on higher loads would be prioritised as these are deemed to have more risk of overloading the supply. The measurement data would suggest that weak grid system startup should instead prioritise the highest inrush loads on startup to improve EMC. In this case the non-linear loads.

CONCLUSION

Islanded microgrids, which do not have the virtually unlimited capacity of network infrastructure, often experience EMI failures due to inrush currents or load switching transients. In this paper inrush current analysis is performed on multiple switching load events occurring under various load conditions. Measurements confirm that power supplies

are electromagnetically interfered by large inrush currents due to non-linear loads charging up, especially during the peak of the voltage sinusoidal waveform, but prediction of supply shutdown remains unpredictable as failure events do not always show a clear distinction from non-failure events. The intermittent nature of inrush current related interference is apparent with certain events which do not disrupt the supply equal or exceeding events which do cause system interference. Increasing the average nominal load may increase the risk of interference but the largest factor remains the nature of non-linear devices connected to the supply as well as the phase firing angle on the voltage waveform that the load is energised. Multiple system failures occurred with a nominal load of only 250 W connected to a supply rated at 5 kVA with the failure rate increasing with a higher average load connected. The use of unregulated non-linear loads require extreme over-dimensioning of power supplies and even so it may not be sufficient. Certain events show vulnerability of a system to inrush current failure but the intermittent nature of the failure remains a challenging problem to diagnose.

REFERENCES

[1] R. Singh and M. Kirar, "Transient stability analysis and improvement in microgrid," *International Conference on Electrical Power and Energy Systems, ICEPES 2016*, no. i, pp. 239–245, 2017.

[2] R. Belkacemi, S. Zarrabian, A. Babalola, and R. Craven, "Experimental Transient Stability Analysis of MicroGrid systems: Lessons learned," *IEEE Power and Energy Society General Meeting*, vol. 2015-Septe, pp. 1–5, 2015.

[3] A. Elsebaay, M. A. Abuadma, and M. Ramadan, "Analyzing the Effect of Motor Loads and Introducing a Method for Selection of Electric Generator Power Rating," *2018 20th International Middle East Power Systems Conference, MEPCON 2018 - Proceedings*, pp. 7–12, 2019.

[4] B. Have, N. Moonen, and F. Leferink, "On-Site Efficiency Analysis of a Generator in the Millisecond Range," pp. 1–4.

[5] F. Leferink, "Conducted interference, challenges and interference cases," *IEEE Electromagnetic Compatibility Magazine*, vol. 4, no. 1, pp. 78–85, 2015.

[6] MIL-STD-1399-300-2, "MEDIUM VOLTAGE ELECTRIC POWER, ALTERNATING CURRENT," *DEPARTMENT OF DEFENSE*, 2018.

[7] R. B. Timens, F. J. K. Buesink, V. Ćuk, J. F. G. Cobben, W. L. Kling, and F. B. J. Leferink, "High harmonic distortion in a new building due to a multitude of electronic equipment," *IEEE International Symposium on Electromagnetic Compatibility*, pp. 393–398, 2011.

[8] C. Keyer, R. Timens, F. Buesink, and F. Leferink, "DC pollution of AC mains due to modern compact fluorescent light lamps and LED lamps," *IEEE International Symposium on Electromagnetic Compatibility*, pp. 632–636, 2013.

[9] V. Ćuk, S. Bhattacharyya, J. F. Cobben, W. L. Kling, R. B. Timens, and F. B. Leferink, "The effect of inrush transients on PV inverter's grid impedance measurement based on inter-harmonic injection," *Renewable Energy and Power Quality Journal*, vol. 1, no. 8, pp. 567–572, 2010.

[10] I. Quesada, A. Lázaro, C. Raga, A. Barrado, R. Vázquez, I. González, and N. Herreros, "Closed loop operation of the harmonic cancellation technique," *IECON Proceedings (Industrial Electronics Conference)*, pp. 607–611, 2008.

[11] J. He, Y. Jun, B. Gong, J. Lei, Y. Liu, and F. Long, "Analysis of start-up inrush current and its mitigation control strategy for grid connected voltage source inverter," *IEEE Transportation Electrification Conference and Expo, ITEC Asia-Pacific 2014 - Conference Proceedings*, pp. 7–10, 2014.

[12] D. T. Viet, N. H. Hieu, N. Le Hoa, and N. M. Khoa, "A control strategy for dynamic voltage restorer," *Proceedings of the International Conference on Power Electronics and Drive Systems*, vol. 2015-Augus, no. June, pp. 1106–1110, 2015.

[13] B. S. Yogananda and K. Thippeswamy, "Design of power filters to improve power quality in power systems," in *2017 International Conference on Energy, Communication, Data Analytics and Soft Computing, ICECDS 2017*. IEEE, 2018, pp. 1953–1956.

[14] M. Danilovic, F. Luo, L. Xue, R. Wang, P. Mattavelli, and D. Boroyevich, "Size and weight dependence of the single stage input EMI filter on switching frequency for low voltage bus aircraft applications," *15th International Power Electronics and Motion Control Conference and Exposition, EPE-PEMC 2012 ECCE Europe*, pp. 4–10, 2012.

[15] V. Zhuikov and K. Osypenko, "The stability of solar panel-diesel generator system," *2016 2nd International Conference on Intelligent Energy and Power Systems, IEPS 2016 - Conference Proceedings*, pp. 2–5, 2016.

[16] A. Matthee, N. Moonen, and F. Leferink, "Sub-Millisecond Transient Analysis with Multi-Point Measurement in Weak Grids," pp. 1–6, 2020.

[17] B. T. Have, T. Hartman, N. Moonen, and F. Leferink, "Misreadings of Static Energy Meters due to Conducted EMI caused by Fast Changing Current," *2019 Joint International Symposium on Electromagnetic Compatibility, Sapporo and Asia-Pacific International Symposium on Electromagnetic Compatibility, EMC Sapporo/APEMC 2019*, pp. 445–448, 2019.